LA-UR- 91-6910

c.1

Title: THE EVOLUTION OF HIGH TEMPERATURE GAS SENSORS

Author(s): FERNANDO H. GARZON, 102961, MST-11
ERIC L. BROSHA, 109937, MST-11
RANGACHARY MUKUNDAN, 120748, MST-11

Submitted to: PHILA ELECTROCHEMICAL SOCIETY MEETING
MAY 13-17, 201ST MEETING

Los Alamos
NATIONAL LABORATORY

Form 836 (8/00)

The Evolution of High Temperature Electrochemical Gas Sensors

Fernando H. Garzon, Eric L. Brosha, and Rangachary Mukundan,

Los Alamos National Laboratory
Electrochemical Materials and Devices Group
Los Alamos, New Mexico 87545

Abstract

Gas sensor technology based on high temperature solid electrolytes is maturing rapidly. Recent advances in metal oxide catalysis and thin film materials science has enabled the design of new electrochemical sensors. We have demonstrated prototype amperometric oxygen sensors, nernstian potentiometric oxygen sensors that operate in high sulfur environments, and hydrocarbon and carbon monoxide sensing mixed potentials sensors. Many of these devices exhibit part per million sensitivities, response times on the order of seconds and excellent long-term stability.

Introduction

The sensing of gases in high temperature environments is of great value for combustion efficiency monitoring and control and also provides feedback data for associated emissions abatement technologies. Combustion processes typically emit hydrocarbon gases, carbon monoxide, nitrogen oxides and nitric oxides. Most industrial nations strickly limit the emission of these effluent gases due to their adverse environmental impacts. Electrochemical sensor technology based on high temperature solid electrolyte materials offers great promise at meeting the aforementioned sensor needs.

High temperature electrochemical gas sensor technology has evolved continously over the last 40 years. Recent advances in thin and thick film materials science, surface science, catalysis and electrochemistry have enabled the development of sensors for many more analyte gases than previously thought possible. Contemporary reviews by Miura [1] and Menil[2] provide detailed descriptions of the development of the technology. The Electronic and Electrochemical Materials and Devices Group at Los Alamos National Laboratory is actively developing new high temperature sensors prototypes to meet sensing needs in the energy and transportation technology sectors of the economy. The goal of this article is to briefly review high temperature electrochemical gas sensor research and describe the ongoing efforts at Los Alamos.

Amperometric Sensors

Electrochemical sensing technologies operate in either a potentiometric mode or an amperometric mode. The amperometric sensors operate on the principle of diffusion-limited electrochemical pumping. The amperometric devices are configured to produce a

mass transport limitation of the analyte gas to the electrode /electrolyte reaction sites thus making the device current sensitive to the gas concentration [3]. The diffusion limited mass transport obey's Fick's and Faraday's laws:

$$J = D_{gas}\frac{\partial C}{\partial x}$$

$$I = nFJA$$

Where J is the flux of the gas in moles/cm^2-sec, I is the device current in amperes, F is Faraday's constant, n is the the number of charges transferred for the reaction, D_{gas} is the diffusion coefficent of the gas, A is the diffusion area and P_{gas} is the partial pressure of the gas. At high pumping potentials, P_{gas} at the electrode -electrolyte interface is very low and thus:

$$\frac{\partial C}{\partial x} = \frac{P_{gas}}{L}$$

$$\therefore I_{\text{limiting}} = \frac{nFD_{gas}P_{gas}A}{L}$$

Where L is the diffusion length, the sensing electrode thickness. The current output of these device increases linearly with increasing oxygen concentration under suitable temperature and applied polarization voltages. Figure 1 illustrates the ideal response of an amperometric sensor.

The limitation of the diffusion of the electroactive species to the electrode-electrolyte boundary may be produced by:

a) The application of an aperture cap over the sensing electrode . Figure 2 illustrates the sensor geometry

b) The use of a diffusion limiting porous overcoat [4] deposited on the sensing electrode.to limit the flux of oxygen to the platinum pumping electrode. A schematic diagram of this sensor is shown in figure 3

c) A dense electrode structure that transports the analyte species to the electrolyte/electrode interface via chemical diffusion [5]. The flux of a species through an ionic and electronic conductor is given by:

$$J = \frac{\sigma_i}{nF}\nabla + D\frac{\partial C}{\partial x}$$

if σ_e is large, $\nabla = 0 \;\therefore\; J = D\frac{\partial C}{\partial x}$

Where ∇ is the electric potential gradient across the sensing electrode, σ_i. σ_e are the ionic and electronic conductivites of the electrode material. The sensing electrode materials selected for this application must have a sufficiently high electronic conductivity so that the flux of oxygen is driven only by a chemical potential gradient. Figure 4 Illustrates a sensor of this type and Figure 5 displays the response to varying oxygen concentrations for sensor made from $La_{0.8}Sr_{0.2}MnO_3$ a perovskite material that has a much greater electronic conductivity than ionic conductivity. Figure 6 is the response behavior of a sensor based on $Zr_{0.46}Y_{0.18}Tb_{0.36}O_{2-x}$ a fluorite mixed conductor whose ionic and electronic conductivities are the same order of magnitude. In this case the flux is potential

dependent due to electric potential gradient driven oxygen migration within the electrode structure.

Potentiometric sensors

The potentiometric devices can be broadly divided into sensors that operate under conditions of thermodynamic equilibrium and devices that rely on selective catalysis and thus are non-equilibrium devices. The non-equilibrium devices are also known as mixed potential devices as the electrode potential is determined by both the equlibirium potentials and the kinetic reaction rates of multiple redox reactions.

Potentiometric sensors that rely on thermodynamic equilibrium have been extensively described by Weppner [6]. Weppner created three classifications to catagorize sensors that operate under thermodynamic equilibrium conditions:

Type I

The first high temperature electrochemical gas sensors were orginally devices that sensed a chemical potential gradient of the species conducted by the solid electrolyte across a gas tight membrane. This class of device requires that thermodynamic equilibrium be established at the gas-solid electrolyte-electrode interface. The most ubiquitous example of this technology is the two-compartment yttria doped zirconia oxygen exhaust gas sensor, a device that typically uses porous platinum electrodes to catalyze thermodymamic equilibrium between diatomic oxygen gas and the oxygen ion conductor:

$$O_{2(g)} + 4e^- \underset{pt}{\longleftrightarrow} 2O^{=}_{(electrolyte)}$$

The response of these devices at thermodynamic equilibrium obey the Nernst equation:

$$E = \frac{RT}{4F} \ln \frac{P_{O_2}^{unknown}}{P_{O_2}^{reference}}$$

Where F is Faraday's constant, R is the ideal gas constant, and T is the device temperature in degrees Kelvin. Figure 7 is a schematic illustration of a two compartment Nerstian sensor.

Porous platinum electrode zirconia sensors are employed in a wide variety of environments; the stability of the platinum electrodes is generally very good. Two exceptional gases where platinum electrodes lack stability are environments where the temperatures exceed 800 C and electrode sintering occurs with a concurrent loss of triple phase boundary area and environments where high sulfur concentrations are present. Typical lifetimes are less than one week for operation in percent levels of sulfurous gases. Replacement of the platinium electrodes with sulfur tolerant refractory electronically conducting oxides greatly improves the sensor lifetime. We have found that terbia doped yttria stabilized zirconia electrodes offer great tolerance to high sulfur environments [7]. The device operated in a paper pulp recovery boiler that produced sulfur containing gas concentrations of 12% for over 500 hours

The lack of suitable electrolytes has limited the sensing of gases using this method to a relatively small group of diatomic molecules, H_2 O_2, Cl_2, and F_2. Other methods must be used to extend the number of detectable gases by high temperature electrochemical techniques

Type II

A second method of making equilibrium is to use a reaction between the gas phase and mobile ions to produce the electrolyte phase. As the activity of the electrolyte phase is constant, the activity at constant temperature of the mobile ion is fixed by gas-ion reaction.

An example of a sensor of this type is the sulfur dioxide sensor developed by researchers at Hydro-Quebec[8]. The device uses an akali metal sulfate such as potassium sulfate as the electrolyte:

Pt, SO_3O_2 /K_2SO_4/ Pt,SO_3,O_2

The cell reaction in these devices is

$$2K^+ + SO_3 + \frac{1}{2}O_2 + 2e^- \Leftrightarrow K_2SO_4$$

Type III

Potentiometric devices can also be fabricated using an auxillary phase to fix the moble ion activity to the gas concentration. An example of a sensor of this type is

O_2 Au/(Na^+)Nasicon/$NaNO_2$/Au,NO_2,O_2[9]

The cell reaction being:

$$Na^+ + NO_2 + e^- \Leftrightarrow NaNO_2$$

In these devices the sodium ion activity is fixed by the reaction of sodium ions with nitrogen dioxide and oxygen to form sodium nitrite.

A limitation of the devices that use auxillary thermodynamic equilibria as the sensing mechanism is a relatively slow time response. It is difficult to acheive thermodynamic equilibrium quickly between the solid and gas phases at modest operating temperatures (300-500 °C). It is also very difficult if not impossible to design equilibrium devices that are sensitive to hydrocarbons.

Mixed potential devices

Electrochemical devices that utilize selective electrocatalysis to produce mixed potentials have been demonstrated to sense a variety of hydrocarbon gases, [] carbon monoxide, hydrogen and nitric oxides[]. An example of a sensor of this type is carbon monoxide sensor that uses two dissimilar electrode materials deposited onto a ytrria stabilized zirconia oxide ion conducting electrolyte. Upon exposure to oxygen and carbon monoxide the following reactions occur on the gas/electrode/electrolyte triple phase boundaries:

$$O_2 + 4e^- \leftrightarrow 2O^{2-}$$
$$CO + O^{2-} \rightarrow CO_2 + 2e^-$$

The mixed potential is established when the electron transfer rates of the oxygen reduction reaction (1) and the carbon monoxide oxidation reaction (2), are equal. Since these reactions occur at different kinetic rates on the dissimilar electrodes a potential difference is established. The successful design of sensors of this type requires the selection of electrode materials with large differences in electrocatalytic rates for the gases sensed. The mixed potential, E_0 of an electrode A or B where multiple redox

reactions are occurring is determined by the activities, a (partial pressures of the gases under typical sensor conditions) of the redox species, O_j, R_k and the reaction rate constants k_{ri} :

$$\sum u_{ij} O_j + n_i e^- \rightarrow \sum v_{ik} R_k$$

$$E_0 = \frac{RT}{nF} \ln \frac{\sum k_{ri} \prod a_{O_j^{u_{ij}}}}{\sum k_{oi} \prod a_{R_k^{u_{ik}}}}$$

$$\Delta E_{sensor} = E_0^A - E_0^B$$

Devices that operate on mixed potential mechanisms typically produce output voltages that are much greater than what would be predicted by thermodynamic equilibrium.
It is often more convienent to express the reaction kinetics for mixed potential devices in terms of the redox current densities, an experimentally measureable quantity in many cases. We have performed experiments of carbon monoxide mixed potential sensors equipped with reference electrodes (figure 8) and determined the mixed potential for carbon monoxide electro-oxidation reactions on each electrode surface displayed in fiigure 9. [10,11]. It was also determined that the differences in the oxygen reduction rates between platinum and gold electrodes was the primary source of the mixed potential not the difference in carbon monoxide electrooxidation rates as postulated by Williams et al [12]. Large differences in oxygen reduction rates between the two electrodes can be readily seen in the polarization plot illustrated in figure 10.
Miura has developed a theoretical analysis of the response of mixed potential devices operating under tafel type electrode kinetics [13]. We have extended the analysis to include electrode kinetics under mass transport limitations and low electrode overpotentials [14].
Most mixed potential sensors use yttria-stabilized zirconia as the solid electrolyte. We have demonstrated that cerium oxide electrolytes may produce devices with superior sensing characteristics particularly at low temperatures [15]. The use of metal oxide electrodes has greatly extended the number of species sensed by mixed potential techniques We have used recently developed physical vapor deposition methods to produce a variety of perovskite and fluorite oxide electrode based hydrocarbon sensors. Figure 11 illustrates a lanthanum manganate electrode, yttria stabilized zirconia electrolyte terbium doped yttria stabilized zirconia sensor and figure 15 illustrates the sensor response to varying levels of propylene. Note the excellent return to base line when the analyte gas is turned off before switching to a new level. Sensors of this type have exhibited excellent response stability for over a thousand hours of testing.

References

1. N. Miura, G. Lu and N Yamazoe Solid State Ionics 136-137 533-542 (2000)
2. F Menil, V Coillard, and C Lucat Sensors and Actuators B 67 1-23 (2000)
3. H. Dietz, Solid State Ionics 6 175-183 (1982)
4. K. Ishibashi, T. Kashima, A, Asada, Sensors and Actuators B 13 41-44 (1993)
5. F. Garzon, I. Raistrick, E. Brosha, R. Houlton, B.Chung, Sensors and Actuators B 50 125-130 (1998)
6. W. Weppner, Sensors and Actuators B 12 107-119 (1987)
7. E.L.Brosha, R. Mukundan, D. Brown, F. Garzon and B. Farber, Solid State Ionic Devices, Proceeding Volume 99-13, The Electrochemcial Society, 374-381 (1999)
8. Chamberland,. J. Gauthier, Atmospheric Environment; 11, 257-61 (1977)
9. S. Yoa, Y, Shimizu, N. Miura, N. Yamazoe, Chem. Lett ,4 587-590
10. R. Mukundan, E.. Brosha, D. Brown, and F. Garzon. *Electrochemical and Solid-State Letters,* **2**, 412-414 (1999).
11. . R. Mukundan, E. Brosha, D. Brown, and F. Garzon. *J. Electrochem Soc* **147,** 1583-8 (2000)
12. D. E. Williams, P. McGeehin and B. C. Tofield, Proc. Second European Con., Solid State Chemistry, Veldhoven, The Netherlands, June 7-9, 275 (1982)
13. N. Miura, T. Raisen, G. Lu, N. Yamazoe, Sensors Actuators B 47 84.-91(1998)
14. F. Garzon, E Brosha and R. Mukundan, Solid State Ionics **136-137** 633-638 (2000)
15. E.Brosha, R. Mukundan, D. Brown, F. Garzon, J. Visser, .M. Zanini, Z. Zhou,

E. Logothetis, Sensors and Actuators B (Chemical); 10 Sept. 2000; vol. B69, no.1-2, p.171-82

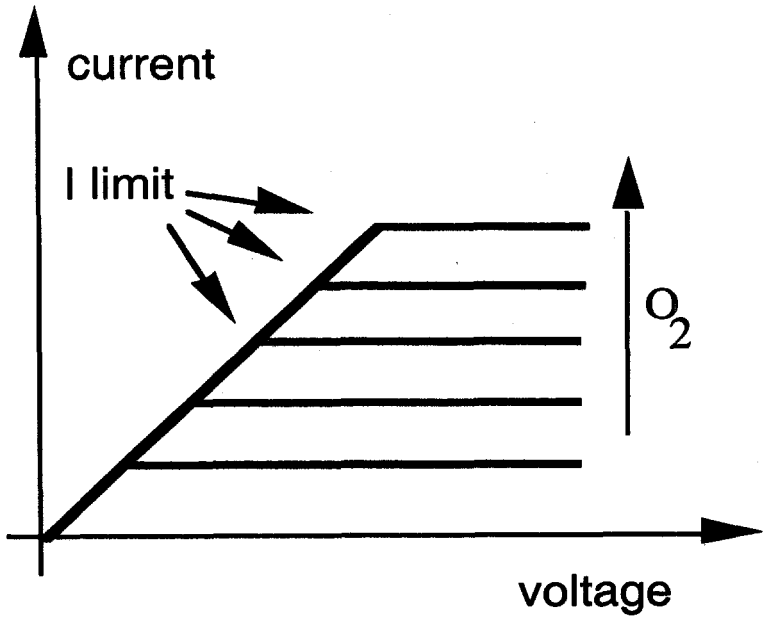

Figure 1 Ideal limiting current oxygen sensor behavior as a function of gas concentration

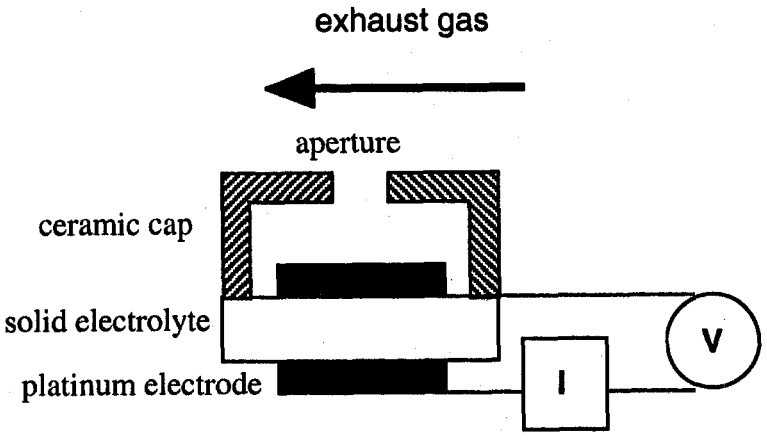

Figure 2. Schematic illustration of a cross-sectional view of an aperture type limiting current sensor [5]

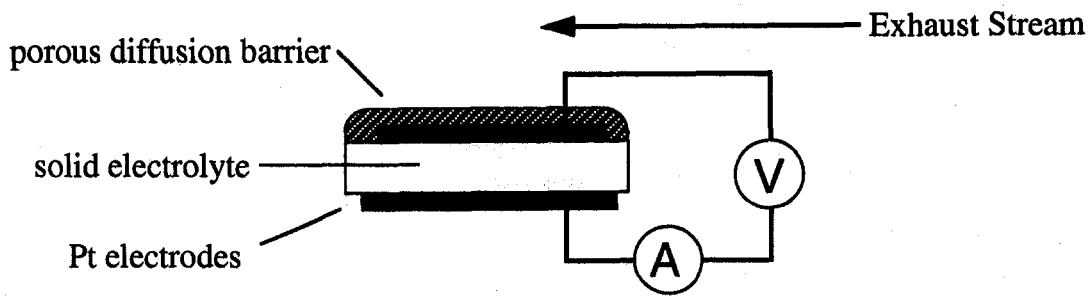

Figure 3. A porous coating diffusion barrier type limiting current sensor. [5]

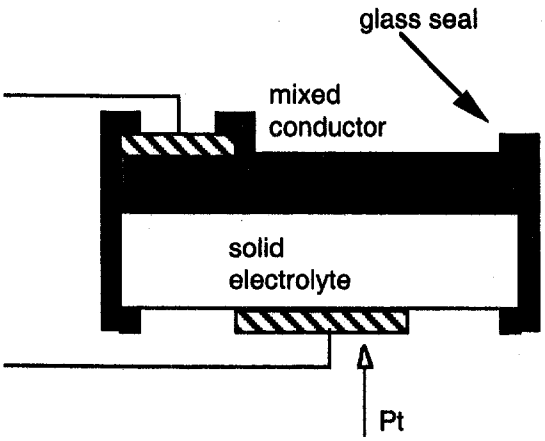

Figure 4 A schematic diagram of a dense diffusion barrier amperometric sensor.[5]

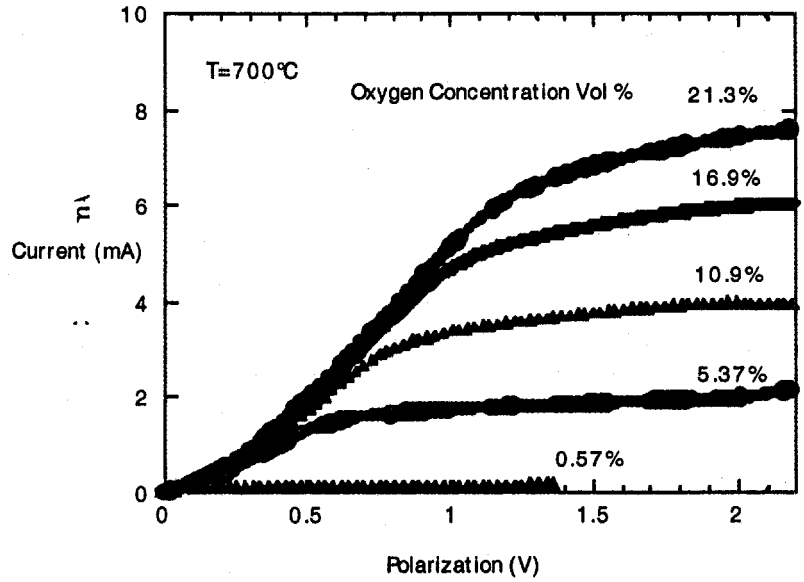

Figure 5. I-V data for sensors based on $La_{0.8}Sr_{0.2}MnO_3$ diffusion barrier film deposited on yttria stabilized zirconia [5]

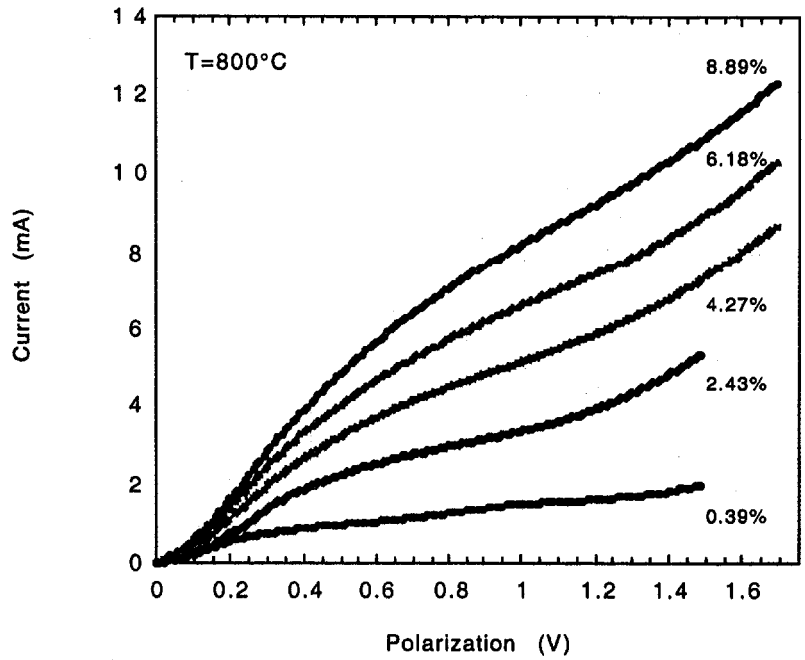

Figure 6. The current voltage response of a $Zr_{0.46}Y_{0.18}Tb_{0.36}O_{2-x}$ electrode yttria stabilized zirconia electrolyte sensor for varying concentrations of oxygen.

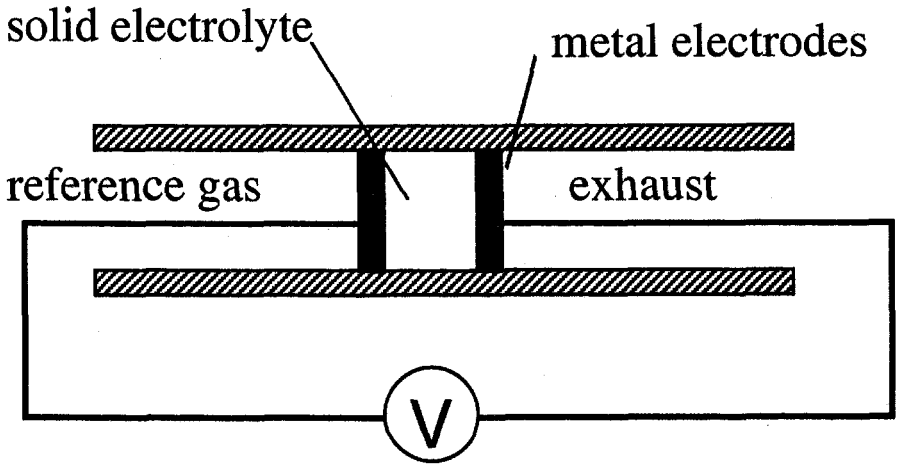

Figure 7. Schematic illustration of a two compartment nernstian sensor cell

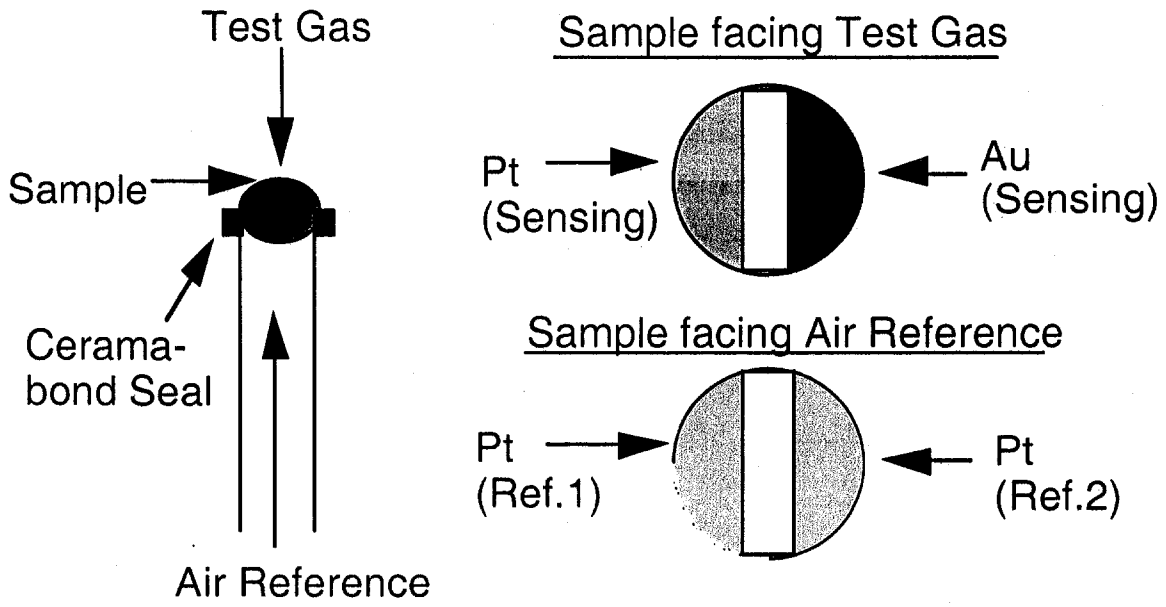

Figure 8 Configuration of a Pt/gadolium doped cerium oxide/Au sensor equipped with Pt air reference electrodes.

T = 600oC
90% response
time < 45sec

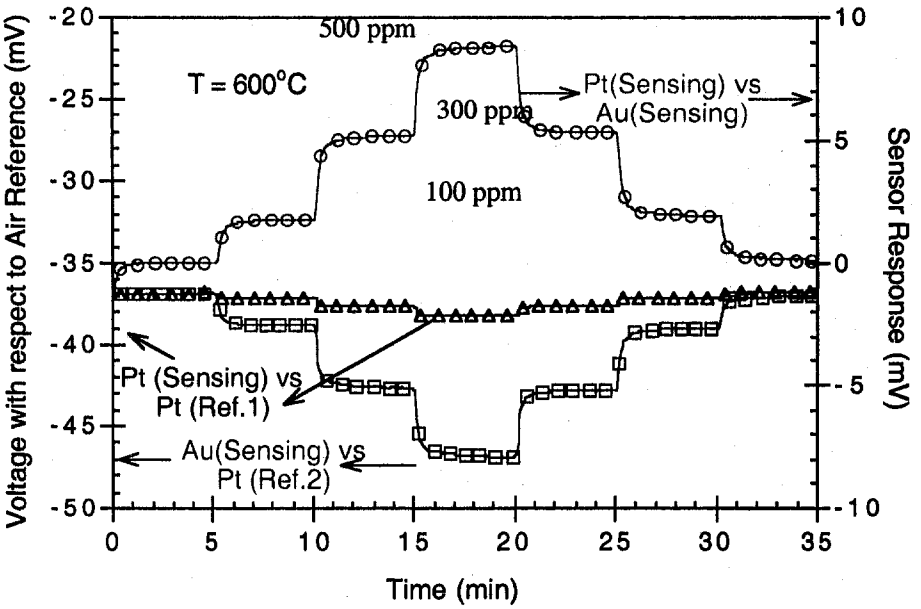

Figure 9 Response of sensor described in figure 8. Top curve is the sensor response the bottom curves are the individual electrode responses. Note the mixed potential arises mostly from the gold electrode.

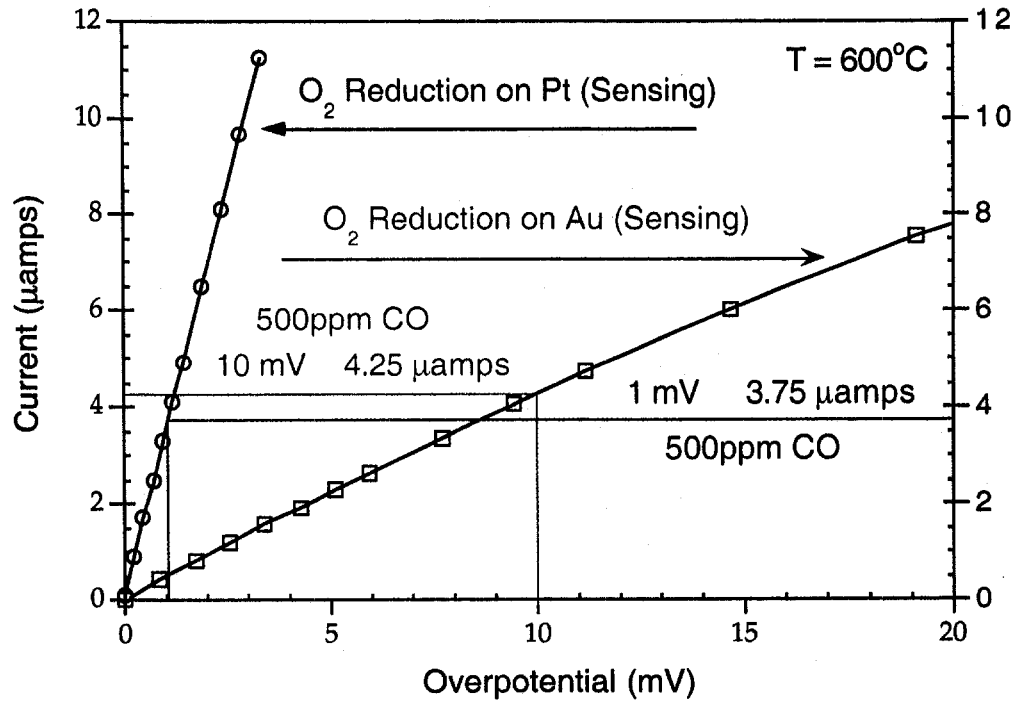

Figure 10 Oxygen reduction versus overpotential data for the sensor illustrated in figure 8. The dashed line represents the mixed potential current for the Pt electrode and the dotted represents the mixed potential current for the gold electrode. The individual electrode mixed potentials were determined from the meausrements against air reference electrodes.

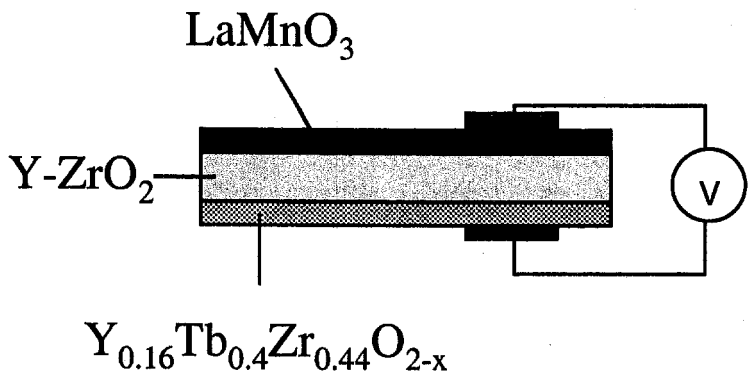

Figure 11. Dual oxide electrode mixed potential sensor

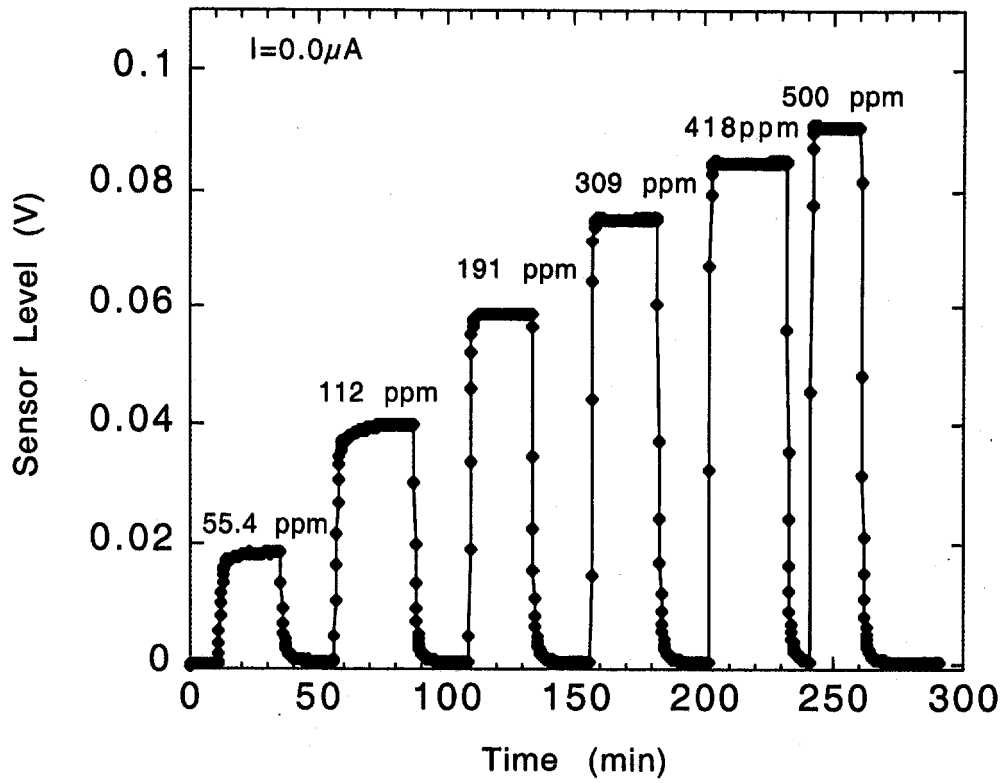

Figure 12. Dual metal oxide sensor response to varying concentrations of propylene gas.